THE UNIVERSITY OF MICHIGAN

COLLEGE OF ENGINEERING
Department of Naval Architecture and Marine Engineering

Final Report

RESEARCH IN RESISTANCE AND PROPULSION

Part III. Blockage Correction in a Ship Model Towing Tank and Scale Effect on Propulsive Parameters

Hun Chol Kim
James L. Moss

Project Director: R. B. Couch

ORA Project 04542

under contract with:

MARITIME ADMINISTRATION
U.S. DEPARTMENT OF COMMERCE
CONTRACT NO. MA-2564, TASK 1
WASHINGTON, D.C.

administered through:

OFFICE OF RESEARCH ADMINISTRATION ANN ARBOR

March 1963

ACKNOWLEDGMENTS

I would like to thank Dr. F. C. Michelsen and James L. Moss for reviewing the manuscripts. Dr. Michelsen has written the part on wave resistance in restricted water.

Hun Chol Kim

TABLE OF CONTENTS

BLOCKAGE CORRECTION IN A SHIP MODEL TOWING TANK

Hun Chol Kim

TABLE OF CONTENTS

LIST OF FIGURES

INTRODUCTION

When dimensions of a towing tank cross section is such that the restriction to the flow of water around a model (as compared to the flow in an unlimited body of water) is measurable, the effect of this restriction is usually referred to as the boundary effects. It may be further classified into Wall Effect, Shallow-depth Effects, and Blockage Effects.

Wall effect refers to the case when the width of the tank is limited but not the depth. A combination of limited width and depth is known as the Blockage Effect. In the highspeed range $(\frac{V}{\sqrt{L}} > 1.0)$ the wall effects become rather complex due to the interference of the walls in regard to the free wave-pattern. Such effects may be named the Reflected Wave Interference Effects.

Benjamin Franklin's investigations on canal navigation are the first records we have on research dealing with resistance of ships in restricted waters. J. Scott Russell[1] must be given the credit, however, as being the first investigator to attempt a physical explanation for the phenomena of increased ship resistance due to blockage effects. Since Scott Russell discussed the problem in 1839, a great many papers on the subject have appeared in the literature. Some of the most significant of these contributions are those of Kreitner,[24] Schlichting,[23] Kinoshita,[2,20] Srettensky,[14] Inui,[12] Hancock,[15] and Hughes.[17] Many others are given in the list of references of this report.

In spite of the great efforts that have been put into research on the problem of restricted water effects we must admit that it is far from completely solved. This is pointed out by the recommendations of

the 1957 International Towing Tank Conference which included the study of the influence of tank boundaries on model resistance. Following this recommendation a great deal of experimental investigations have been performed, in particular in Great Britain.(3,4)

The phenomena of Blockage Effect is rather complex and an exact analytical solution is yet to be derived. Of course, the degree of completeness required in an analysis will depend on the accuracy called for. In this case the accuracy must be a function of the amount of increase in model resistance due to blockage in per cent of total resistance. Unfortunately it can be said that although it has long been recognized that blockage effects have existed in many tanks, they have quite frequently been neglected, or some rough estimate of their magnitude may at the most have been made. Countless numbers of towing data therefore suffer from blockage effects in various degrees, and this very fact tends to obscure another very important issue, namely that of scale effect.

The most important parameter governing the blockage effect is that of blockage ratio. Blockage ratio is simply defined as the ratio of the maximum cross sectional area of the model to that of the towing tank. The lower limit of blockage ratio below which the blockage effect has normally been considered to be negligible is 0.006. Results of experimentation at the University of Michigan, as shown in Section II, indicate however, that in addition to blockage ratio both the speed-length ratio and the block-coefficient play an important role in the determination of the blockage effect.

At the inception of self-propulsion testing at the University of Michigan the model sizes were chosen to be 14 feet, in order to avoid

serious scale effect on the propeller performance. The first three self-propulsion tests were made with Series 60 forms of block-coefficients C_B = .60, .75, and .80. The blockage ratio for these models ranged from .0072 to .0100, and since these values were relatively high it became a necessity to consider blockage effects very seriously.

A fairly complete study of existing literature was undertaken. It was found that due to differences of approach and also the way in which the various authors introduced their boundary conditions it became natural to divide their works into five categories. In the following sections are included an outline of each of these and also the details of some experimental work on the subject conducted at the University of Michigan.

I. SURVEY OF LITERATURE

A. J. Kreitner's Analysis of Resistance of Ships in Restricted Waters[24]

Bernoulli's equation applied to sections at a midship of the model and ahead of it gives

$$\rho g h_o + \frac{\rho}{2} v_o^2 = \rho g h + \frac{\rho}{2} (v_o + \Delta v)^2 \qquad (1)$$

By equation of continuity

$$S_o v_o = (S_o - a - b\Delta h)(v_o + \Delta v) \qquad (2)$$

Solving Equation (1) for $h_o - h = \Delta h$, and substituting into Equation (2) (For notations, see Appendix A.) we obtain the following cubic equation,

$$\left(\frac{v_o + \Delta v}{v_o}\right)^3 \left(\frac{F^2}{2}\right) - \left(\frac{v_o + \Delta v}{v_o}\right)\left[1 - \frac{a}{S_o} + \frac{F^2}{2}\right] + 1 = 0 \qquad (3)$$

where

$$F^2 = \frac{v_o^2}{gh}$$

$$\frac{a}{S_o} = \text{blockage ratio}$$

A plot of Equation (3) for different values of $\frac{a}{S_o}$ is shown in Figure 1. It is noted that there is a region of speed in which no real solution of the cubic equation exists. This is called the critical speed region, and the lower and upper speed regions are called sub-critical and super-critical regions, respectively. For a model going through these speed regions, notable changes are observed. These are explained in detail in Appendix A.

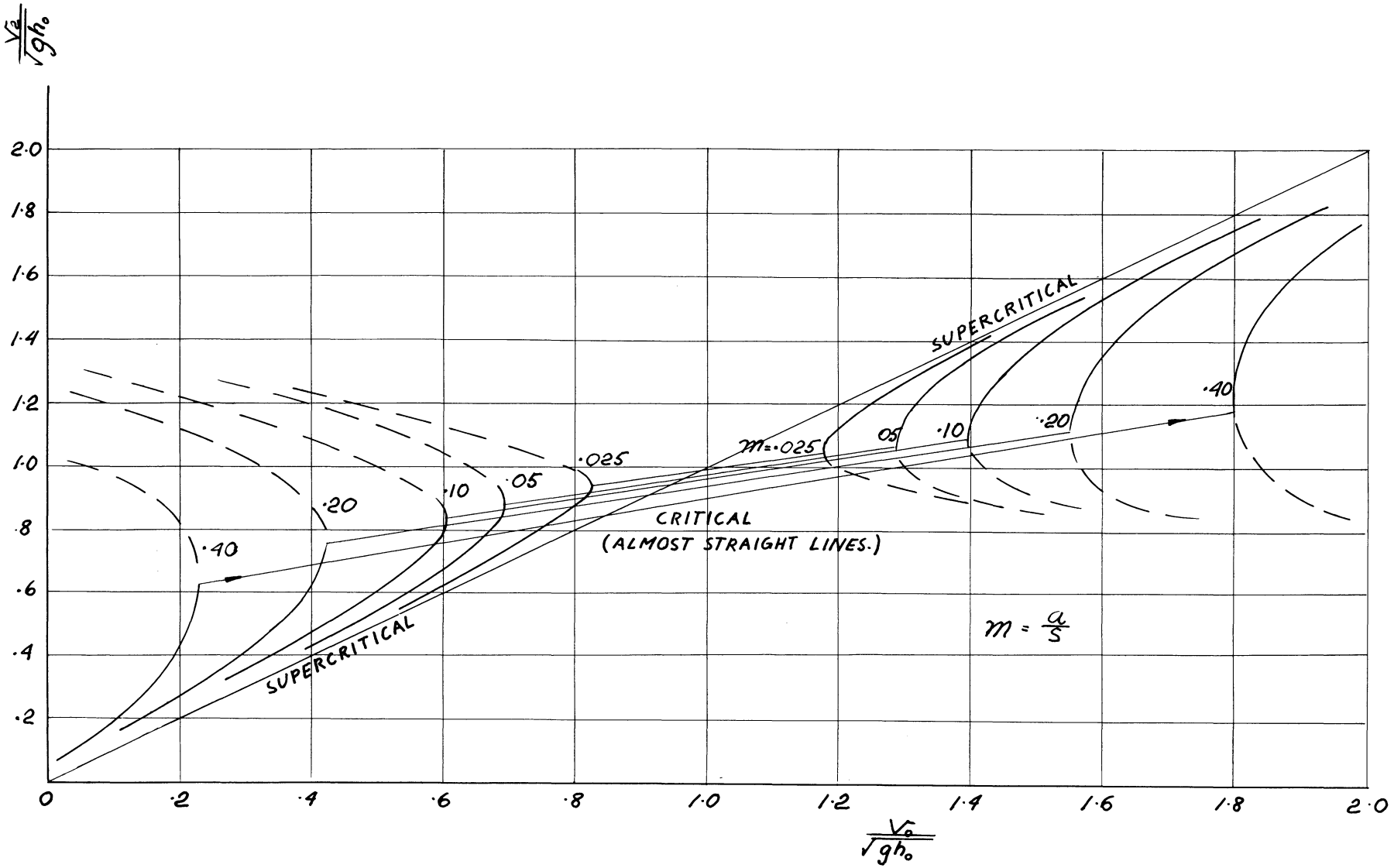

Figure 1. Speed increase alongside a model (Kreitner's analysis). (Depth Froude number of flow around the model vs. depth Froude number based on model speed.)

Simplified versions of Equation (3) result in

$$\frac{\Delta v}{v} = \frac{m}{1-m-F^2} \; ; \quad m = \frac{a}{S_o} \tag{4}$$

$$\frac{\Delta h}{h} = F^2\left(\frac{\Delta v}{v}\right) \tag{5}$$

Late works by Kinoshita,[2,11] G. Hughes,[3] and A. Emerson[4] are experimental verification of Kreitner's Equations (4) and (5) above. H. Maruo[5] extended the analysis to two dimensions, which resulted in a non-linear equation of two variables. T. Constantine attempted an analysis at the critical speed and published various graphs.[6]

B. O. Schlichting's Hypotheses[23]

On the basis of the results of several hundred model tests performed for the German Navy, Schlichting offered two hypotheses for explaining the increase in resistance of ships moving in shallow waters.

The first hypothesis may be stated in these terms: "For a ship traveling at a given speed in shallow water, the amplitude, length, and form of the waves are equal to the wave generated by the same ship in deep water at a 'corresponding' speed."[26] The second hypothesis is that the increase in velocity of the potential flow in shallow water arises from the restriction of the section available for the reverse flow.

The condition of equal wave resistances yields, as shown in Appendix B, the following relationship between speeds in deep and shallow water at the same wave amplitude and wave length:

$$\frac{v}{v_\infty} = \frac{v_\infty - \Delta v}{v_\infty} \quad \left[\tanh\left(\frac{gh_o}{v_\infty^2}\right)\right]^{\frac{1}{2}} \tag{6}$$

However, there are doubts about the validity of the first hypothesis. Visual observation of wave forms, on which the hypothesis was based, can hardly be quantitatively correct since small differences in wave characteristics which must have been present were not taken into account. Furthermore, in deep water the spectrum of frequencies of waves generated by a ship is complete and continuous, whereas for a model in a tank, wave frequencies have discrete values. The first hypothesis is therefore not in agreement with physical facts.

Landweber's[8] application of the hydraulic radius principle in the "Clairton" series tests makes use of the same hypothesis.

Weinblum[7] established a criterion based on the ratio of short axis to long axis of the elliptical motion of fluid particles, which, occurs when depth is restricted. It is defined as follows:

$$\frac{\text{short axis}}{\text{long axis}} \simeq \tanh\left(\frac{gh_o}{V_\infty^2}\right) < 0.95 \qquad (7)$$

or $\frac{V}{\sqrt{gh_o}} > 0.74$ for appreciable shallow water effects. The above equation is known as Weinblum's criterion.

C. Method of Array of Images

This method was developed primarily for wind tunnels, and therefore, does not include changes in free surface elevation. Wave-making resistance is also ignored. Additional shortcomings are that no prediction of critical speed range is given and the method fails to give an estimate of squat and trim. Borden's work[9] belongs to this category.

D. Application of Wave-Resistance Theory

The first theoretical work on wall effects, based on Wave-Resistance theory, was done by Srettensky.[14] To satisfy the boundary conditions on the canal walls he considered an infinite number of ships running parallel a distance equal to the canal width apart. The resulting expression for the wave resistance as given by Srettensky was:

$$R = \frac{16\,\pi^2\rho g}{bv^2}\left\{I_o^2 + J_o^2 + 2\sum_{k=1}^{\infty}(I_k^2 + J_k^2)\,\frac{\cosh^2\tau_k}{\cosh 2\tau_k}\right\} \qquad (8)$$

where

$$I_k = \iint_{(s)} F(x,z)\; e^{\frac{g}{v^2}\cosh^2\tau_k z}\cos\left(\frac{gx}{v^2}\cosh\tau_k\right)\,dxdz$$

$$J_k = \iint_{(s)} F(x,z)\; e^{\frac{g}{v^2}\cosh\tau_k z}\sin\left(\frac{gx}{v^2}\cosh\tau_k\right)\,dxdz$$

$$(k = 0,\ 1,\ 2,\ 3\ \ldots)$$

and τ_k are the roots of the equation

$$\frac{gb}{4v^2}\sinh 2\tau = \pi k$$

The summation in Equation (8) represents the increase in wave-resistance due to the presence of the walls. The depth is assumed to be infinite. The publication by Srettensky referred to above contains no numerical results.

A most valuable extension to Srettensky's work was made by Inui and Bessho[12] when they calculated the increase in wave resistance due to tank wall reflections. Applying the formulae for wave-resistance coefficients to the case of a hull form represented by a linear source

distribution given by $m_1 = a_1 \xi$ (S - Series models), Inui[13] arrived at the following equations

(i) Deep Water ($h = \infty$, $b = \infty$)

$$c'_w = \frac{R_w}{\frac{1}{2}\rho v^2 (a_1 L)^2} = \frac{2}{\pi} \int_0^{\frac{\pi}{2}} U_\infty^2 M_\infty^2 \cos\Theta \, d\Theta \qquad (9)$$

where

$$U_\infty = 1 - \exp(-\kappa_o T \sec^2\Theta)$$

$$M_\infty = -\frac{\cos p_\infty}{p_\infty} + \frac{\sin p_\infty}{p_\infty}$$

$$p_\infty = \kappa_o \ell \sec\Theta; \quad \kappa_o = \frac{g}{v^2}$$

(ii) Unrestricted Shallow Water (h = finite, $b = \infty$)

$$c'_w = \frac{2}{\pi} \int_{\Theta_o}^{\frac{\pi}{2}} U_h^2 \cdot M_h^2 \frac{\cosh^2\alpha}{\frac{1}{2}\sinh 2\alpha - \alpha} \cos\Theta \, d\Theta \qquad (10)$$

where α is the real root of the equation

$$\frac{\tanh \alpha}{\alpha} = F_h^2 \cos^2\Theta \; : \; F_h = \frac{v}{\sqrt{gh}}$$

and

$$U_h = \frac{\sinh(h) - \sinh[\alpha(1 - \frac{T}{h})]}{\cosh \alpha}$$

$$M_h = -\frac{\cos p_h}{p_h} + \frac{\sin p_h}{p_h}$$

$$p_h = \alpha(\frac{\ell}{h}) \cos\Theta$$

The lower limit of the integral of Equation (10) is given by

$$\Theta_o = \cos^{-1}(\frac{1}{F_h})$$

One notes that $\frac{\partial c_w'}{\partial F_h}$ is discontinuous at $F_h = 1$

iii) Restricted Shallow Water (h and b finite)

$$c_w' = 2\kappa_o h(\frac{h}{b})[\frac{U_{h,o}^2 M_{h,o}^2}{D_o} + 2 \sum_{h=1}^{\infty} \frac{U_{h,n}^2 M_{h,n}^2}{D_h}] \qquad (11)$$

where

$$U_{h,n} = \frac{\sinh \alpha_n - \sinh(\alpha_n - \frac{T}{h})}{\cosh \alpha_n}$$

and

$$M_{h,n} = \frac{\sin p_{h,n}}{p_{h,n}^2} - \frac{\cos p_{h,n}}{p_{h,n}}$$

with

$$p_{h,n} = \alpha_n (\frac{L}{2h}) \cos \Theta_n$$

α_n and Θ_n are given by

(a) $\alpha_n^2 \sin^2\Theta_n = 4n^2\pi^2(\frac{h}{b})^2$

(b) $\alpha_n^2 \cos^2\Theta_n = \alpha_n \kappa_o h \tanh \alpha_n$

from which

$$\alpha_n^2 - \alpha_n \kappa_o h \tanh \alpha_n = 4n^2\pi^2(\frac{h}{b})$$

It should be noted that, to the approximation of the Michell wave-resistance theory, Inui is defining the source strength such that for the particular case in question

$$a_1 \xi = -2 \frac{\partial_y(\xi, \zeta)}{\partial \xi}$$

c_w' as given by Equation (11) also shows discontinuity at $F_h = 1$. This discontinuity is such that for $F_h > 1$ the wave-resistance in shallow

water is lower than that in deep water. When $F_h < 1$ this situation is generally reversed. It is interesting to note from computed values presented by Inui,[13] however, that in the range of Froude number of $.3 < F < .33$ the wave resistance in shallow water ($\frac{h}{L} = .2$, $b = \infty$) is also less than for deep water. It appears therefore that the blockage effects on wave resistance may be negative or positive over a speed range of practical interest. Many more theoretical calculations will have to be made before more general conclusions can be reached, but it is important to realize that the wave-resistance theory predicts the existence of humps and hollows in the blockage correction factor. Results presented in this report also show that this has been verified experimentally.

The increase in frictional resistance due to blockage must be expected to be monotomically increasing with speed. Provided the amplitude of oscillations of the wave-resistance blockage effects are sufficiently large, it can therefore be expected that over a certain speed range the total blockage effect may be a decreasing function of speed.

Frequently wave resistance theory neglects high order terms, and for a model in the tank system, boundary conditions on the hull may not be satisfied due to the presence of reflected image systems unless higher order terms are included. Dr. L. Landweber, during his recent stay at the University of Michigan, suggested a method of including the second order term by an iteration process and by solving Fredholm integral equations.[28] Such an analysis is under consideration at the University of Michigan.

E. Empirical Methods

There is a variety of empirical expressions, to which category all previous experimental determinations of blockage factors belong. Figures 2 and 3 compare actual data with some of the expressions as used by various tanks for models UM 912 and UM 913. The following list is included for completeness only.

1) Telfer, E. V.[18]

$$\Delta R = C_2 \Delta v - \beta \Delta \left(\frac{a}{S-a}\right) \tag{12}$$

where

R = Froude's contour of resistance;
a and S = defined earlier;
β = blockage factor;
C_2 = const.

2) Hughes, G.[17]

$$\Delta c_t = c_t - c_{t\infty} = p c_f + q c_r \tag{13}$$

where p and q are functions of a/S, blockage ratio, but not functions of scale ratio and Reynolds number.

$$\Delta c_t = 1.6 \frac{a}{S} c_f + 16 \frac{a}{S} c_r \tag{14}$$

for Victory Ship Series.

3) Cedric Ridgely-Nevitt.[16]

Increase

$$c_f\left(\frac{.066}{(\log_{10} Re - 2.03)^2}\right)$$

by 60% for Victory ships
by 35% for Liberty ships

$$\frac{\Delta R}{R} = n_t \frac{\Delta v}{v}$$

Blockage ratio $m = .720 \times 10^{-2}$

Prismatic $\bar{m} = .434 \times 10^{-2}$

$m' = \frac{m+\bar{m}}{2} = .572 \times 10^{-2}$

(Tank: 21'-2" x 8'-6" = 190 sq ft)

1 Hughes: $k \frac{\delta v}{v}$

2 Emerson: $\frac{\delta v}{v} = 1.65 \frac{m'}{1-m'-F_h^2}$

3 Japan: $\frac{\delta v}{v} = 1.1\, m \left(\frac{L}{b}\right)^{3/4}$

4 Hughes: $\frac{\delta v}{v} = \frac{\bar{m}}{1-\bar{m}-F_h^2}$

5 Landweber: $\frac{\delta v}{v} = \sqrt{\tan h\left(\frac{1}{F_h^2}\right)}\, \Phi\left(\frac{v_o}{r}\right) - 1$

6 Hughes: $\frac{\delta v}{v} = \frac{\nabla_m}{A^{3/2}}$

7 n_t

8 Necessary amount $\frac{\delta v}{v}$ (approx.)

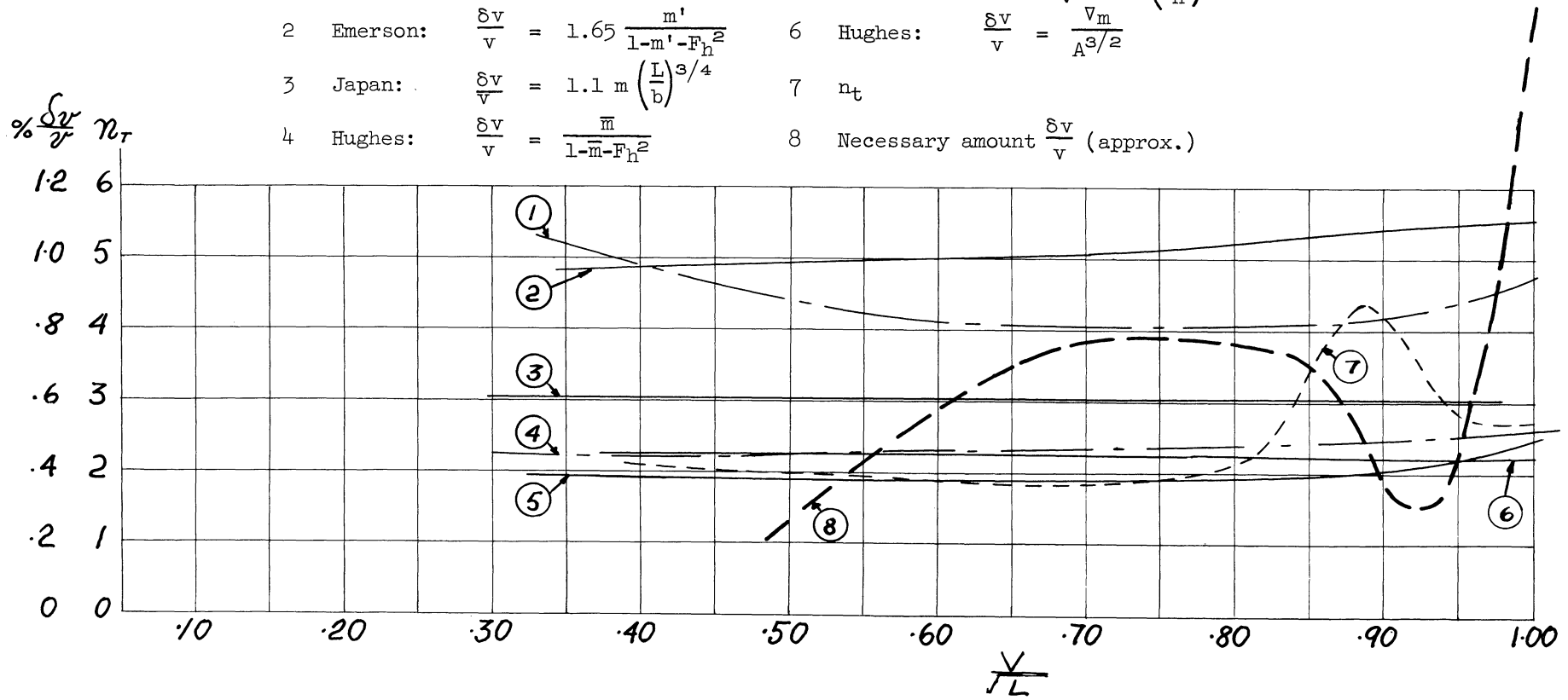

Figure 2. Comparisons of various methods of blockage corrections applied to UM Model 912, $C_B = .60$.

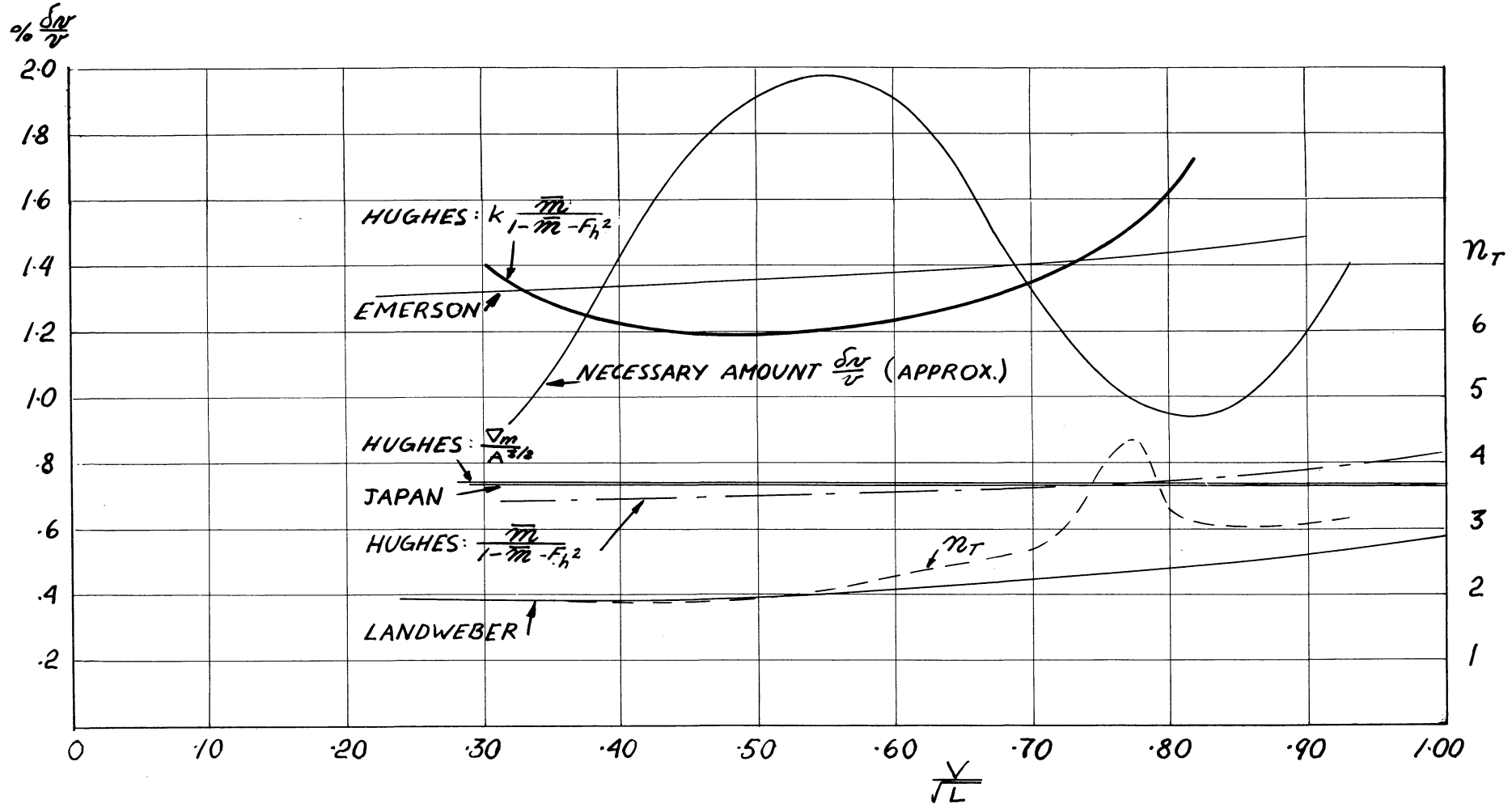

Figure 3. Comparison of various methods of blockage corrections applied to UM Model 913, C_B = .75. m = .891 x 10^{-2}; $\bar{m}$ = .670 x 10^{-2}; m' = .781 x 10^{-2}.

for speed-length ratios between 0.50 and 0.75. Corrections are to be made when blockage ratios exceed the following values.

0.006 for Victory type full ship

0.003 for high speed ship such as destroyer

0.001 for planning craft.

4) Mitsubishi Towing Tank, Japan.

$$\frac{\Delta v}{v} = 1.1\left(\frac{a}{S}\right)\left(\frac{L_m}{b}\right)^{3/4} \tag{15}$$

5) Nagasaki Towing Tank, Jampan

$$\frac{R + \Delta R}{R} = 1 + 3.0985\left(\frac{a}{S}\right) + 10.928\left(\frac{a}{S}\right)^2 \tag{16}$$

6) S. Shoichi.[27]

$$\frac{c_f - c_{f\infty}}{c_{f\infty}} = 191.4\left(\frac{\sqrt{a}}{h} - 0.32\right) + 16.6\left(\frac{\sqrt{a}}{h} - 0.32\right) \tag{17}$$

for shallow bed condition (from trial data).

Returning to J. Kreitner's method, the predicted value of speed increase by Equation (4) is found not always equal to the actual difference obtained from experiments. This is to be expected, since there are a number of simplifications in the derivations of the equations. A correlation factor defined as:

$$k = \frac{\text{actual value of } \frac{\Delta v}{v}}{\frac{\Delta v}{v} \text{ given by Eq. (4)}}$$

was used by Dr. Hughes in plotting some 73 model test data from two tanks of N.P.L.[3] The result is not exactly encouraging because of large scatter when k is plotted against Froude number. (See Figure 2 of

Dr. Hughes' paper.). The mathematical mean of all k shows oscillatory values, and when humps and hollows are leveled, it can be reduced to:

$$k = 32.13(F)^2 - 15.56F - 3.64$$

where F is Froude number based on length.

Dr. Hughes suggests that an average value of $k = 1.7$ be used for normal merchant forms.

II. METHOD EMPLOYED AT THE UNIVERSITY OF MICHIGAN

At the University of Michigan, a procedure similar to Dr. Hughes' has been adopted. Data from David Taylor Model Basin have been used as the basis, although there are probably small blockage effects not accounted for included in these. DTMB data were reduced to UM model size by the 1947 ATTC friction extrapolator. Differences in the two curves of resistance, the actual Michigan data and the converted DTMB data, were read off in terms of speed correction as shown in Figure 4 for three Series 60 models. Differences in resistance were

$$\frac{\Delta R_T}{R_T} = n_T \frac{\Delta v}{v}$$

where n_T for three Series 60 models is shown in Figure 5. Figure 6 indicates the result of Equation (4) applied to these models. Note here that instead of blockage ratio, a mean blockage ratio $\bar{m} = \frac{\nabla_m}{L_m A_{TANK}}$ has been used. Dividing the curves of Figure 4 by those of Figure 6, the curves of k, Figure 7, were obtained, and a series of curves as functions of $V/\sqrt{LWL}$ and C_B were derived algebraically. The blockage correction in terms of speed increase is added to the carriage speed and corrected speed is used for all calculations. Speed increase is, then,

$$\left(\frac{\Delta v}{v}\right)_{CORRECTION} = k\left(\frac{\Delta v}{v}\right)_{Eq.(4)}$$

There is a remarkable consistency in the actual data points which show oscillatory variations, and the over-all average is close to values found elsewhere. Going back to Dr. Hughes' data, it can be seen that similar oscillations exist in data of individual models.

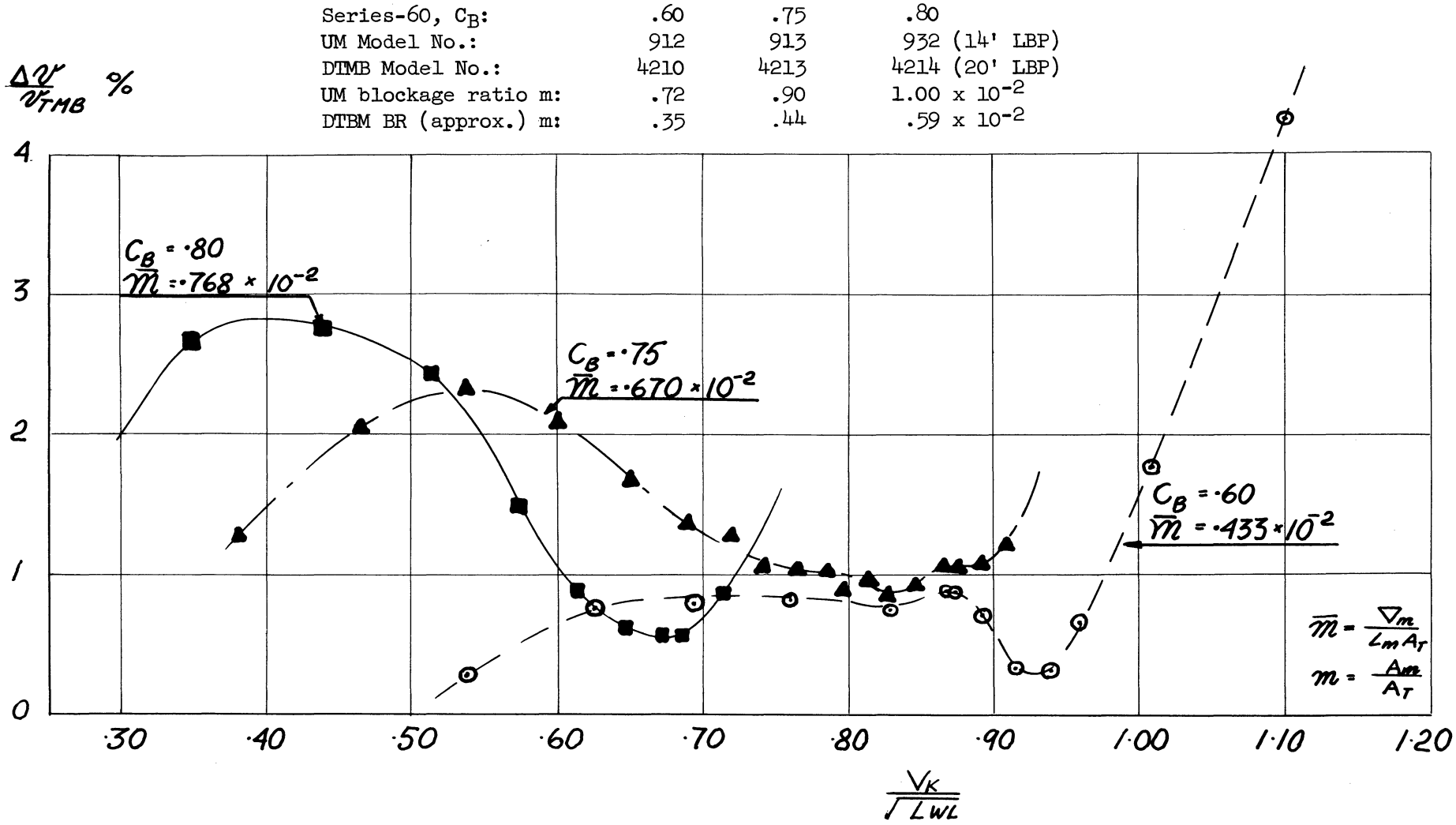

Fig. 4. Necessary amount of speed correction due to blockage for three series-60 models.

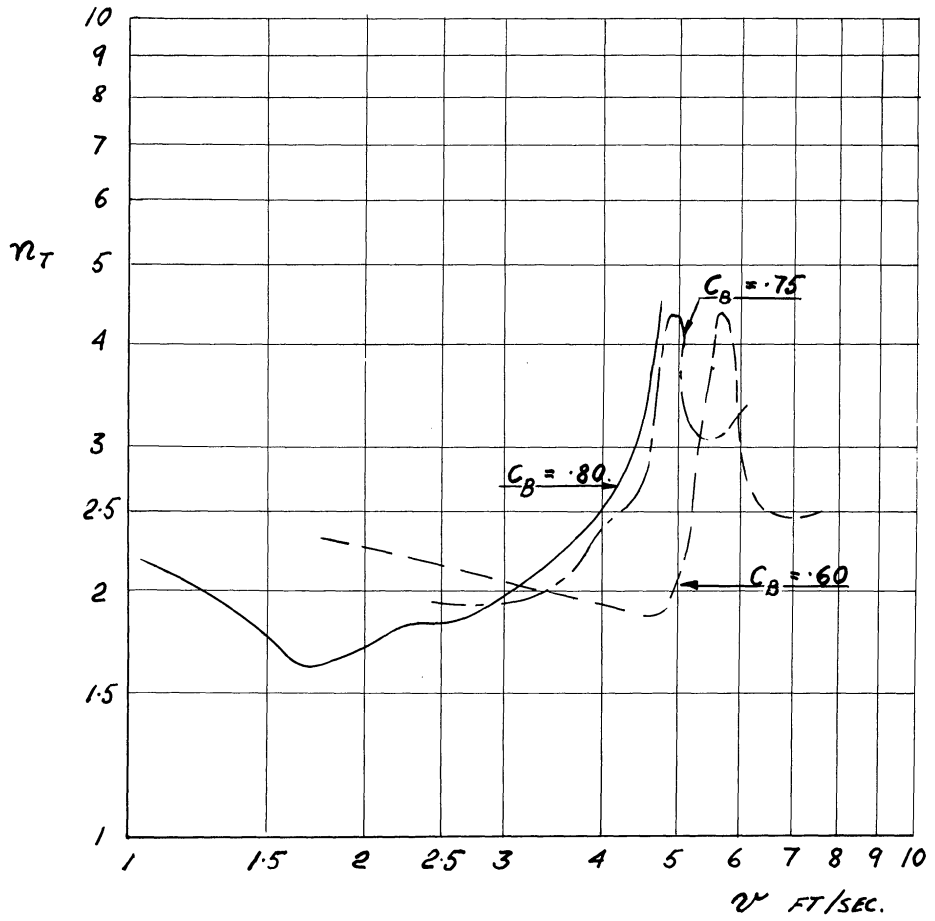

Figure 5. Logarithmic index of model total resistance variation to speed for three series-60 models.

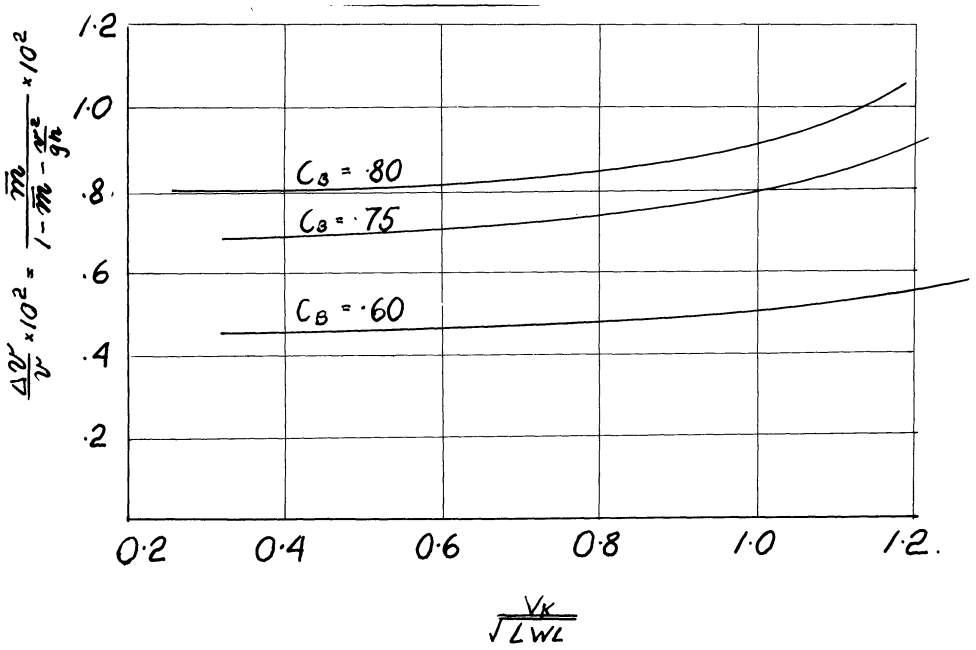

Figure 6. Speed increase on three series-60 models based on one-dimensional analysis.

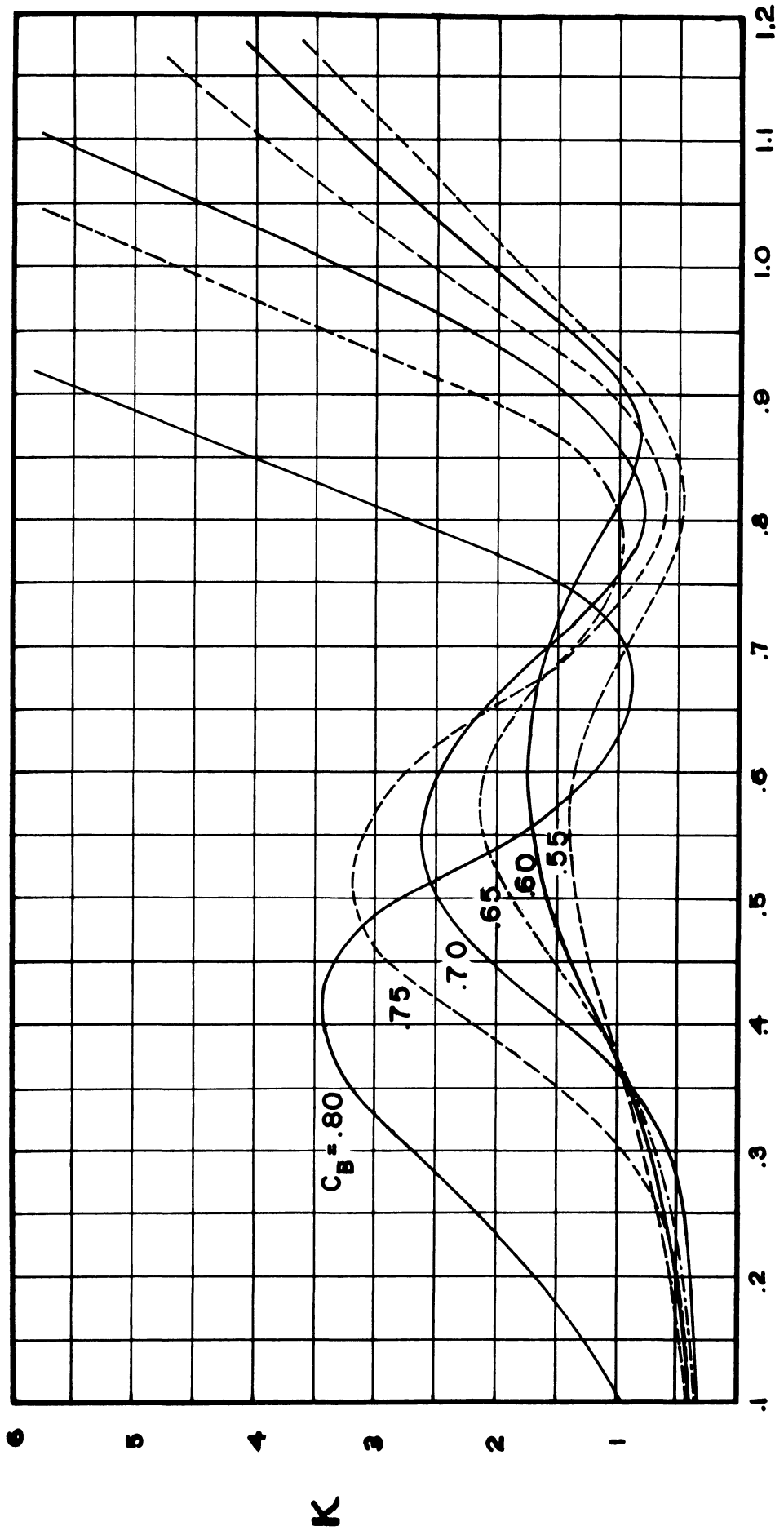

Figure 7. Curve of K-factors used for estimating blockage correction at The University of Michigan.

The University of Michigan towing tank cross section is curved at the bottom and has a trough in the middle.[25] There is a false bottom made of wood, extending 3/5th of the width and about 150 feet of the length, seven feet below the free surface. It is difficult to judge the exact effective area and the depth of the tank, especially depth because the bottom is wooden-planked on a metal frame and the sides are open. At present, pending further analysis, 8.5 feet for depth and 190 square feet for area are being used.

In order to investigate how well the above correlation method predicted blockage effects, the false bottom was raised to 4.0 feet below the surface and UM Model 932, Series 60, $C_B = 0.80$, was tested and its data analyzed as shown in Figure 8. Rather than the actual depth of 4.0 feet, an effective depth estimated at 4.85 feet and a corresponding cross sectional area of 85 square feet was used in the calculation.* The result shows the necessity of further analysis pending further experiments. It is expected that it will be necessary to separate the effects of finite width and finite depth. In order to do so we are planning to install movable tank walls above the false bottom so that the tank cross section can be varied over a wide range of sizes and proportions.

* The estimate of the effective depth was arrived at by a consideration of the fact that the false bottom does not extend completely to the tank walls.

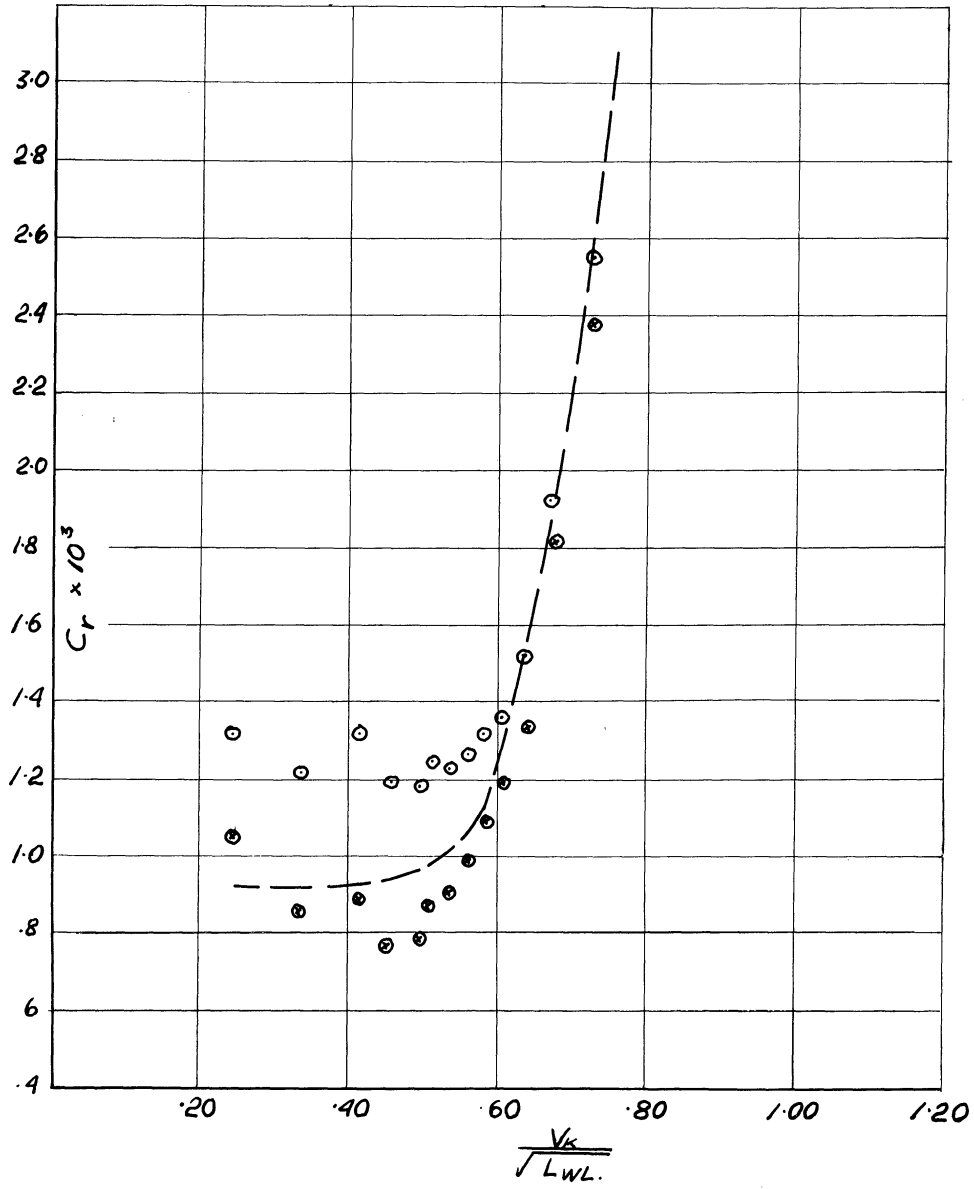

Figure 8. Effect of shallow bed on UM Model 932, C_B = .80.

⊙ : Test data at tank depth of 4.85 ft
⊗ : Same data corrected for blockage effect
— — : Model No. 932 result at U of M (from a deep water test

BIBLIOGRAPHY

1. Russell, J. Scott. "Report on Waves." British Association Reports, 1844.

2. Kinoshita, M. "On Restricted Boundary Effect on Ship Resistance." Transactions of Japan Society of Naval Architects, Vol. 76, pp. 173-213, Sept., 1954. (Read in 1946)

3. Hughes, G. "Tank Boundary Effects on Model Resistance." Transactions of R.I.N.A., 1961.

4. Emerson, A. "Ship Model Size and Tank Boundary Correction." Transactions of N.E.C.E.S., p. 251, Nov. 1959.

5. Maruo, Hajime. "On the Shallow Water Effect." Transactions Japan S.N.A., Nov. 1948.

6. Constantine, T. "On the Movement of Ships in Restricted Waterways." Journal of Fluid Mechanics, pp. 247-256, 1961.

7. Weinblum, G. "Wellenwiderstand auf Beschrankten Wasser." Jahrbuck der Schiffbautechnischen Gesellschaft, Bd. 39, 1938.

8. Landweber, L. David Taylor Model Basin Report, No. 460.

9. Borden, A. "Wall Corrections for Flow about Two- and Three-Dimensional Symmetrical Bodies in Rectangular Channels of Infinite and Finite Lengths." TMB 864, Dec. 1954.

10. Kinoshita, M. "Shallow Bed Effect on Wave Resistance of a Moving Sphere." Transactions Japan S.N.A., Vol. 73, 1952.

11. _____. "Theory and Calculation of Shallow Bed Effect on Wave Resistance of Submerged Spheroid and Normal Ship Forms." (with Takao Inui) Transactions Japan S.N.A., Fall, 1944. (Numerous works by this author are available in Japan.)

12. Inui, T. and M. Bessho. "Side-Wall Effects on Ship Wave Resistance." Transactions Japan S.N.A., Fall, 1952.

13. Inui, T. "Study on Wave-Making Resistance of Ships." Society of Naval Architects of Japan 60th Anniversary Series, Vol. 2, p. 185.

14. Srettensky, L.N. "On the Wave-Making Resistance of a Ship Moving Along in a Canal." Philosophical Magazine, Vol. 22, 1936.

15. Hancock and Comstock. "The Effect of Size of Towing Tank on Model Resistance." Transactions of SNAME, Vol. 50, 1942.

16. Ridgely-Nevitt, C. "Geometrically Similar Models -- An Investigation of Some Problems Resulting from Their Resistance Values." International Shipbuilding Progress, 1957.

17. Hughes, G. "The Effect of Model and Tank Size in Two Series of Resistance Tests." Transactions of R.I.N.A., 1957.

18. Telfer, E. V. "Ship Model Correlation and Tank Wall-Effect." Transactions of R.I.N.A., 1953.

19. Nakamura, S. "Studies on the Hull Forms of Fishing Boats by Systemactic Series Model Experiments." Transactions Japan S.N.A.

20. Kinoshita, M., Y. Yamanouchi, B. Kanda and E. Morisaki. "On the Effect of the Restricted Water Upon the Resistance and Propulsive Performance of Ships." Transactions of Japan Society of Naval Architects, Fall, 1949.

21. Theodorsen, Theodore. "The Theory of Wind Tunnel Wall Interference." NACA Report, No. 410, 1931.

22. Havelock, T. H. "The Effect of Shallow Water on Wave Resistance." Proceedings of Royal Society of London, 1922.

23. Schlichting, O. "Schiffswiderstand auf beschrankter Wassertiefer." Jahrbuch der Schiffbautechnischen Gesellschaft, p. 127, 1934.

24. Kreitner, J. "Uber den Schiffswiderstand auf beschrankter Wasser." Werft Reederei Hafen, 1934.

25. Michelsen, F. C., R. B. Couch and H. C. Kim. "Resistance and Propulsion Tests on Two Series 60 Models." University of Michigan ORA Report No. 03509-1-F, April 1961.

26. Lamenen, Troost and Koning. Resistance, Propulsion and Steering of Ships. Haarlem, Holland: Technical Publishing Co., p. 59, 1948.

27. Shoichi, S. "On the Effect of Shallow Water Upon the Resistance of Large Tankers." Transactions Japan S.N.A., No. 108, 1961.

28. Michelsen, F. C. "Research in Resistance and Propulsion. Part I. A Program for Long-Range Research on Ship Resistance and Propulsion." University of Michigan ORA Report 04542-1-F, February, 1963, Appendix II, p. 67.

APPENDIX A

J. KREITNER'S ONE-DIMENSIONAL ANALYSIS

Assume the coordinate system is fixed with respect to the model, and that the tank boundaries and the water have relative velocity v_o. Let the undisturbed cross-sectional area of the tank have area S_o with breadth b and depth h_o and let the model midship sectional area be a. We can imagine that at the bow of the model the free surface will begin to rise, at the midship the water will attain its maximum speed, the pressure will decrease and the free surface will be lowered. Aft of the model the speed of flow will finally reach v_o and the free surface will be raised to h_o again. Let Δv be the average increment of speed such that $v = v_o + \Delta v$, and let Δh be the mean depression of the water surface such that $h = h_o + \Delta h$.

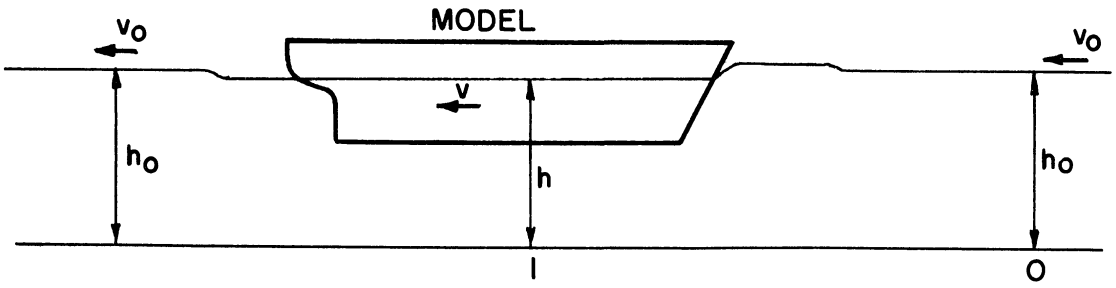

Figure A-1. Coordinate system with a model moving in a channel.

If we apply the continuity equation and Bernoulli's equation between the sections 0 and 1, Figure A-1, we get for continuity:

$$S_o v_o = (S_o - a - b\Delta h)(v_o + \Delta v) \qquad \text{(A-1)}$$

and for Bernoulli's equation:

$$\rho g h_o + \frac{\rho}{2} v_o^2 = \rho g h + \frac{\rho}{2}(v_o + \Delta v)^2 \qquad (A\text{-}2)$$

$$h_o - h = \Delta h = \frac{1}{2g}[(v_o + \Delta v)^2 - v_o^2] \qquad (A\text{-}3)$$

From (1) and (3)

$$S_o v_o = S_o(v_o + \Delta v) - a(v_o + \Delta v) - \frac{b}{2g}(v_o + \Delta v)^3 + \frac{b v_o^2}{2g}(v_o + \Delta v)$$

Dividing by $S_o v_o$, we get

$$1 = \frac{v_o + \Delta v}{v_o} + \frac{a}{S_o v_o}(v_o + \Delta v) - \frac{(v_o + \Delta v)^3}{2g h_o v_o} + \frac{v_o(v_o + \Delta v)}{2g\, h_o}$$

$$\frac{v_o^2(v_o + \Delta v)^3}{2g h_o v_o^3} - \frac{v_o + \Delta v}{v_o} + \frac{a(v_o + \Delta v)}{b h v_o} - \frac{v_o^2(v_o + \Delta v)}{2g h_o v_o} + 1 = 0$$

$$\left(\frac{v_o + \Delta v}{v_o}\right)^3 \left(\frac{F^2}{2}\right) - \frac{v_o + \Delta v}{v_o}\left[1 - \frac{a}{S_o} + \frac{F^2}{2}\right] + 1 = 0 \qquad (A\text{-}4)$$

where

$$F^2 = \frac{v_o^2}{g\, h}$$

This is a cubic equation the solution of which is difficult to find.

Equation (4) can be rewritten as:

$$\frac{v_o}{\sqrt{g h_o}} = \frac{v_o + \Delta v}{\sqrt{g h_o}}\left\{1 - \frac{a}{S_o} - \frac{1}{2}\left[\frac{(v_o + \Delta v)^2}{g h_o} - \frac{v_o^2}{g h}\right]\right\} \qquad (A\text{-}5)$$

If model resistance and squat and trim are measured and plotted, they would show characteristics similar to those shown in Figure A-2.

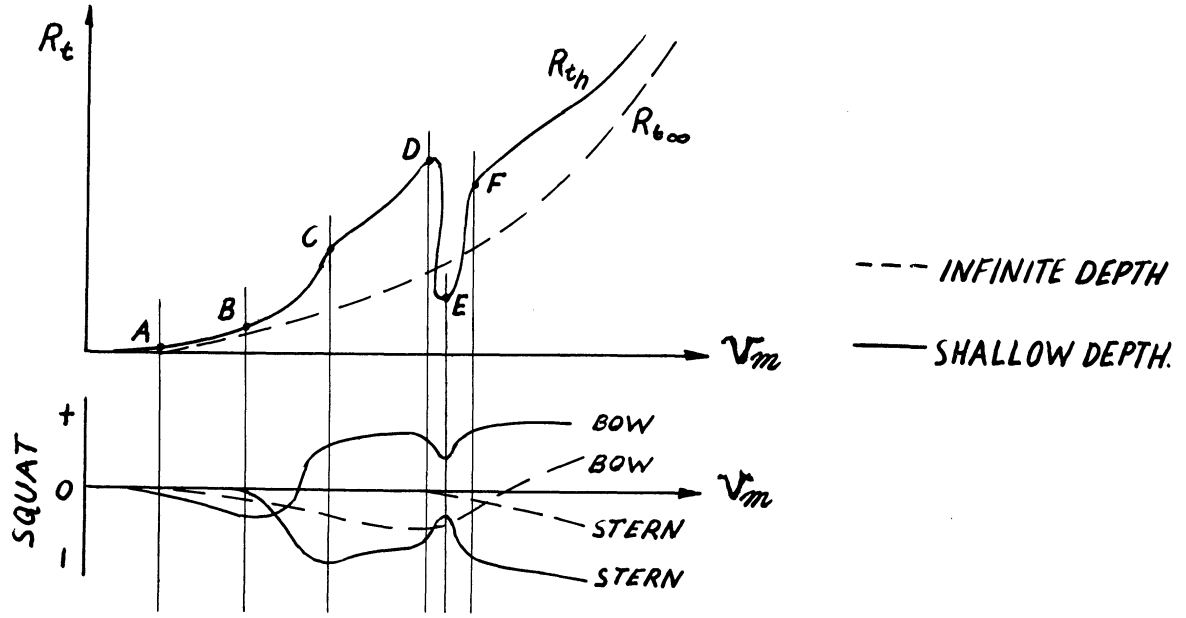

Figure A-2. A typical resistance and squat and trim due to a large blockage ratio.

Points A, B, ..., and F are chosen on the resistance curve and the characteristics of model at each of these speeds may be discribed as follows:*

v_A: Below this speed there is no appreciable blockage effect. It can be seen that this is only true when the speed of the model is zero or the blockage ratio, m, is zero. In the actual case, however, any effects not within the accuracy of experiments may be considered zero.

v_B: As the speed is increased gradually, blockage becomes apparent. Since the volume of flow, $S_o v_o$, must pass by the model and since the flow area is reduced by a, the flow speed increases by Δv. By Bernoulli's law, the water level along the model is lowered by Δh.

* The author is indebted to Dr. Kinoshita for most of these explanations. Reference 20.

Δh depends on the blockage ratio, and increases as the speed of the flow of water around the model increases, and correspondingly, the flow sectional area decreases for increasing Δh.

v_C: It is increasingly difficult, and then impossible, for the flow to increase its speed, and the ability of the flow to pass the bottle-neck reaches a maximum. The speed in this region, v_C, is called the lower limit of the critical speed, and the bore is piled up in front of the model, at which point maximum increment in speed, or in model resistance, is reached. Due to the bore, or hydraulic jump, the water level aft of the model becomes lower than the level at the bow. Also the minimum pressure peak occurs slightly aft of midship. As a result, excessive trim is noted.

v_D: (Maximum-point of resistance) The model tends to overtake the bore as model speed increases such that the water along the model is decelerated. This causes the water level to rise to the still water level and beyond. With the increase of flow area, the bottle-neck phenomenon is relieved.

v_E: When the model speed reaches the solitary wave speed, depth Froude number equals one, in the channel, the model is, in effect, riding with the wave. The ability

of the water to flow through the bottle-neck is high, although the water speed in along the model side is low due to the rise in water level beyond that of the still water. This is the upper limit of the critical speed.

v_F: As the speed is increased the water level no longer rises, but rather lowers, and the flow and model speeds are equal. Super-critical speed has been reached.

To simplify the expression in Equation (A-5), we return to Equations (A-1) and (A-3).

Equation (A-1)

$$S_o v_o = S_o v_o - (a + b\Delta h)v_o - (a + b\Delta h)\Delta v + S_o \Delta v$$

$$\frac{\Delta v}{v_o} = \frac{a + b\Delta h}{S_o - a - b\Delta h} \qquad \text{where} \quad \Delta h\, \Delta v \ll 1$$

$$\simeq \frac{a + b\Delta h}{S_o - a} \tag{A-6}$$

Equation (A-3):

$$\Delta h = \frac{v\Delta v}{g} - \frac{(\Delta v)^2}{2g} \simeq \frac{v\Delta v}{g} \tag{A-7}$$

From Equations (A-7) and (A-6),

$$\frac{\Delta v}{v_o} = \frac{a + \frac{bv_o \cdot \Delta v}{g}}{S_o - a}$$

$$\Delta v\left(S_o - a - \frac{bv_o^2}{g}\right) = av_o$$

$$\frac{\Delta v}{v_o} = \frac{a}{S_o - a - \frac{bv_o^2}{g}} = \frac{m}{1 - m - F^2} \; ; \quad m = \frac{a}{S_o} \tag{A-8}$$

$$\frac{\Delta h}{h} = \frac{v_o \Delta v}{gh} = F^2 \frac{m}{1 - m - F^2} \tag{A-9}$$

APPENDIX B

0. SCHLICHTING'S HYPOTHESIS

From the theory of simple harmonic progressing waves of two dimensions, phase velocity is given by

$$v = \left[\frac{g\lambda}{2\pi} \tanh \frac{2\pi h_o}{\lambda}\right]^{1/2} \tag{B-1}$$

where

λ = wave length

g = gravitational constant

For deep water $\left(\frac{h_o}{\lambda} > \sim 0.5\right)$

$$v_\infty = \left[\frac{g\lambda}{2\pi}\right]^{1/2} \tag{B-2}$$

For shallow water $\left(\frac{h_o}{\lambda} <\sim 0.02\right)$, phase velocity becomes independent of wave length or

$$v_{h_o} = [gh_o]^{1/2} \tag{B-3}$$

The total energy per wave length is given by

$$E = \frac{1}{2} \rho g A^2 \lambda \tag{B-4}$$

where A = wave amplitude

Wave systems generated by ships or models have waves of many wave lengths, in general an infinite number in deep water. In both cases, the wave systems necessarily trail behind the moving pressure point or the model, hence the phase velocity of each component of the wave system must be equal to the velocity of the moving body. The total energy

stored in the fluid is equal to the work done by the pressure point, and work done is equal to the wave resistance multiplied by the speed. Therefore, the condition of equal wave resistances in deep water and in shallow water requires that the energies stored in each case be equal,

$$E_{\infty} = E_{h_o} = \frac{1}{2} \rho g A_{\infty}^2 \lambda_{\infty} = \frac{1}{2} \rho g A_{h_o}^2 \lambda_{h_o} \qquad \text{(B-5)}$$

This condition can be attained if both wave amplitude A, and wave length, λ, are equal simultaneously, conditions which are the first hypothesis of O. Schlichting. The relationship between speed in deep water and that in shallow water is then (from Equation (B-1) and (B-2))

$$\frac{v}{v_{\infty}} = \frac{v_{\infty} - \Delta v}{v_{\infty}} = \left[\tanh \frac{2\pi h_o}{\lambda}\right]^{1/2}$$

$$\simeq \left[\tanh \left(\frac{g h_o}{v_{\infty}^2}\right)\right]^{1/2} \qquad \text{(B-6)}$$

where Δv is the increase in speed in shallow depth water.

SCALE EFFECT ON PROPULSIVE PARAMETERS

James L. Moss

LIST OF TABLES

LIST OF FIGURES

The results of the self-propulsion tests of the three Series-60 models performed at the University of Michigan lend themselves to propulsion parameter scale effect studies when compared with results obtained from 20-foot models tested at DTMB. In general, predicted SHP values compared quite well[9,10] although values of individual propulsion factors did exhibit scale effects.

Although the primary purpose of the testing of the Series-60 models in the University of Michigan tank was to make an over-all comparison between DTMB and University of Michigan data, a detailed analysis of results with emphasis upon scale effects is desirable and pertinent in order to ascertain the relationship between observed scale effects, theoretical predictions and scale effects previously measured elsewhere and reported in the literature.

Throughout the comparatively brief history of self-propulstion model testing inconsistencies in both magnitude and direction in scale effects have been predominant.

Regarding wake fraction, the assumption usually made is that the potential and wave parts are not subject to more than negligible scale effect, but that frictional wake is. One concludes that because of the decreasing nature of the frictional resistance coefficient with increasing Reynolds number, or more exactly, the relative decrease of boundary layer thickness with increasing model size, that frictional wake should also decrease with increasing model size. Unfortunately, however, analysis of test data from model tests and full scale trials is inconsistent. Examples of larger wake on the ship than on the model exist.

The explanation usually given is that the larger relative roughness of the ship tends to thicken the ship boundary layer and increase the wake. However, Hill[1] reports trial results with various hull paints, zinc chromate and hot plastics, which yielded essentially the same wake. Also, in those tests ship wake was four to five points higher than model wake.

Regarding resistance augmentation, the flow velocity over the hull is increased owing to the presence of an operating propeller. Thrust deduction is, then, the additional thrust supplied by the propeller in overcoming the resistance augmentation. An intuitive explanation of scale effect on thrust deduction, based upon logical hypothesis, is not easily forwarded contrary to the case with wake fraction. In fact, in full scale trials tow rope resistance is calculated by means of the assumption that thrust deduction is not subject to scale effect. By means of this assumption roughness corrections to frictional drag are computed although they might better be called correlation factors.

Herein are reported results, both theoretical and experimental, which have been selected in order to best demonstrate the reigning confusion. Multitudes of data exist, but those included are believed to represent results of carefully conducted experiments.

Theoretically, Tsakonas[2,3] has computed thrust deduction and wake fraction, for the airship "Akron" taking into account both potential and viscous effects, by assuming a line singularity distribution for an ellipsoid of revolution and a sink disc for the propeller. For the viscous part three different three dimensional boundary layer theories were tried, those of Millikan, Granville, and Hickling. The results are plotted to a

base of Reynolds number in Figure 1. The potential parts were shown to be heavily dependent upon axial propeller clearance. The clearance chosen here is 0.01L.

Experimentally, the Dutch tests of the victory ship geosim are fairly extensive. Figure 2 shows these results for mean nominal wake plotted analogously to Figure 1 as reported by van Manen and Lap.[4] The curve is a mean line through points for models of from 1/50 to 1/18 scale, all at a speed-length ratio of 0.71. Also shown in Figure 2 is a mean line through the thrust deduction data as reported by van Lammeren, van Manen, and Lap.[5] In this case the scales ran from 1/50 to 1/6 and the original data was plotted over a wide range of speed-length ratios. Also plotted in Figure 2 are the DTMB results for the "Albacore" as reported by Hadler.[6] The ship was towed, deeply submerged, and when propelled the propeller thrust was measured by two independent methods. Agreement between the two methods gave a spread of only about 3% in thrust deduction. Seemingly, then, one can consider the trials as having been carefully conducted. The model was of 1/13.33 scale and was tested in the conventional manner. The results, when compared with the Dutch mean line, indicate scale effect of the same order of magnitude.

Figure 3 shows thrust wake fraction and thrust deduction for the Swedish tests of four victory ship models with scales ranging from 1/17 to 1/28 as reported by Edstrand.[7] Comparison of these results with those of the Dutch and those from the "Albacore" tests exhibits completely opposite trends with regard to scale effect on thrust deduction.

Van Lammeren's[8] test results of the "Simon Bolivar," Figure 4, indicate trends for thrust deduction and wake fraction similar to the Swedish "Victory Ship" results.

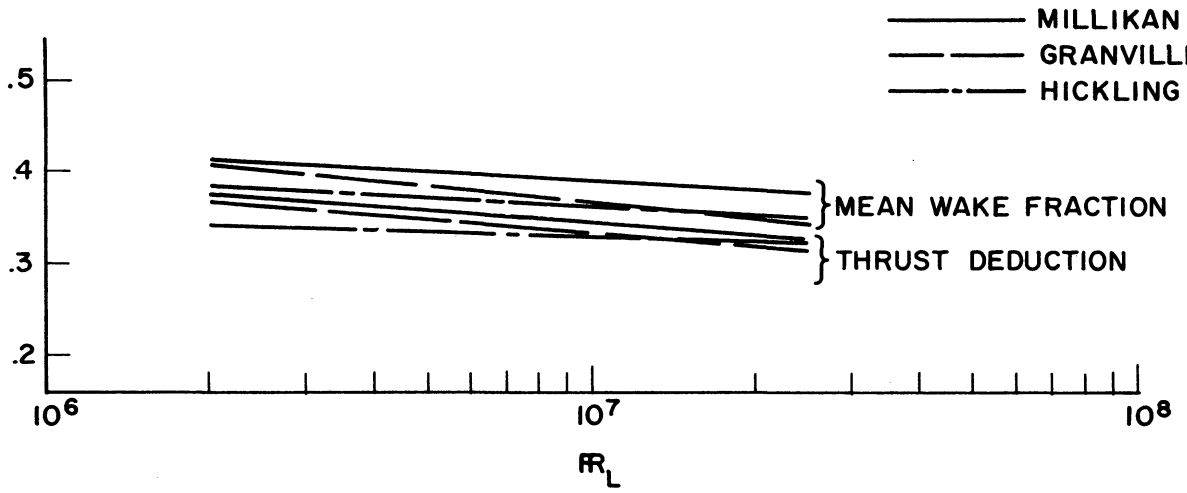

Figure 1. Theoretical results by Tsakonas.

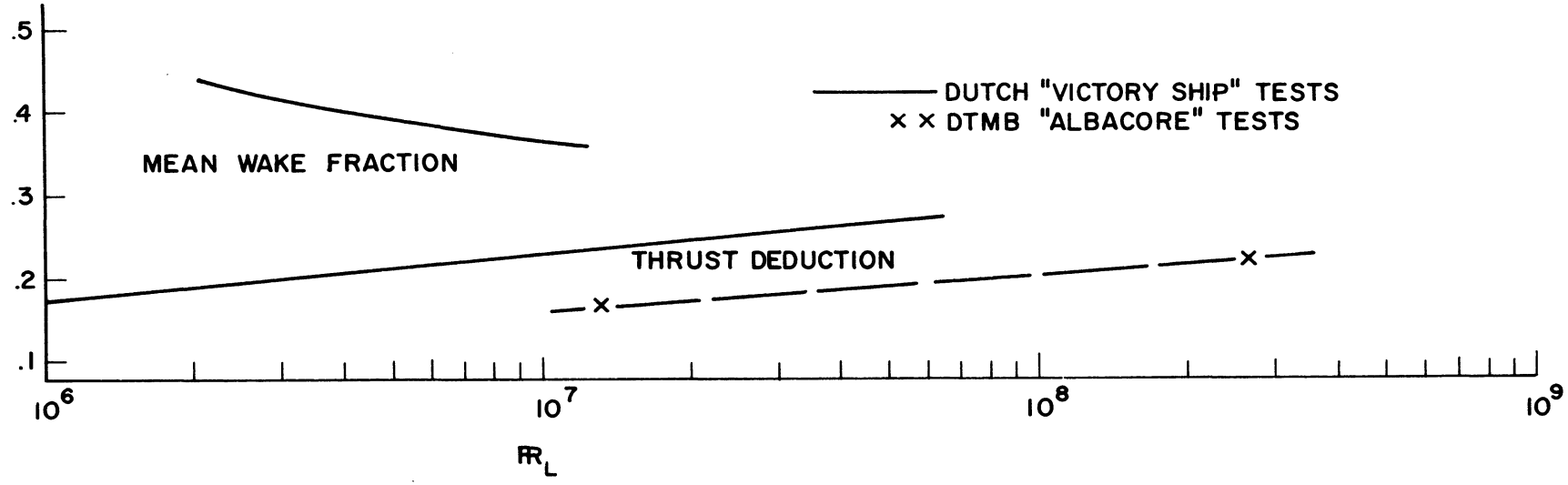

Figure 2. Dutch "Victory Ship" model test and DTMB "Albacore" trial test results.

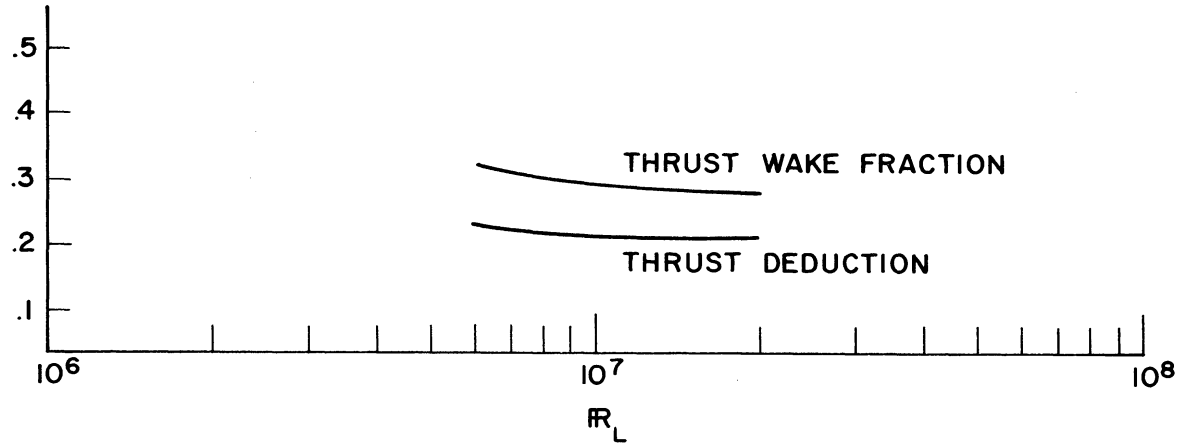

Figure 3. Swedish "Victory Ship" model test results.

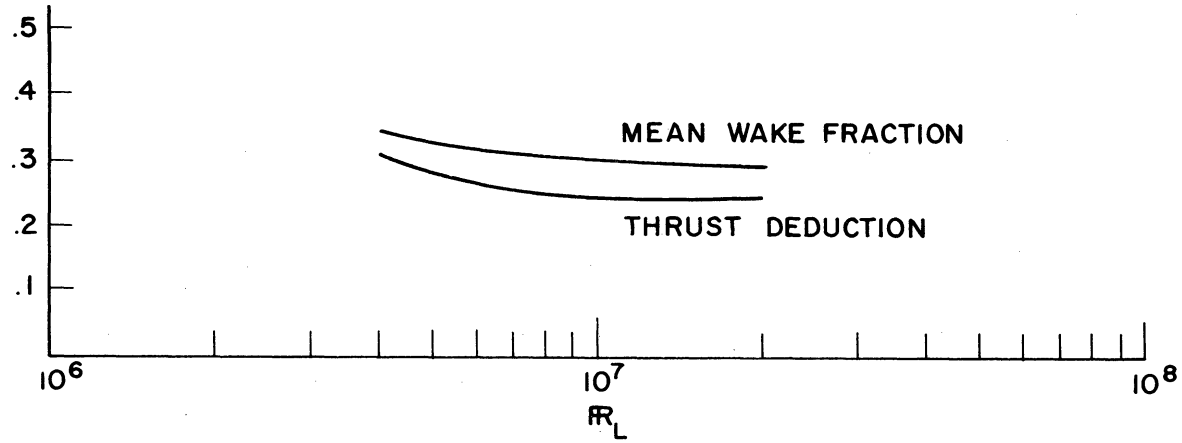

Figure 4. "Simon Bolivar" model test results.

Table I through III give a summary of SHP test results for three Series-60 parents tested at DTMB and Michigan. Wake fraction and thrust deduction from the tables are plotted in Figures 5 and 6, respectively, through which data mean lines have been drawn.

Direct comparisons between the various results presented are made ambiguous because of the many different hull forms involved. Tsakonas has shown that both potential wake and thrust deduction are effected by aperture clearance which is not the same for all the forms compared. Also, one might expect fullness to affect viscous components as separation may be more pronounced with hulls of larger block coefficient. The fact that some tests are run at the model propulsion point and others at the ship propulsion point, and that Froude friction extrapolation in one case and Schoenherr in another have been used, further present difficulty when trying to compare directly. Probably these effects are secondary in nature as is assumed about the potential parts when plotting on a Reynolds number base. In any case, trends for any series of geosim tests should be expected to be the same. Consequently, in Figures 7 and 8 the slopes of the curves already presented are drawn.

In general, with the exception of the Dutch "Victory Ship" and the "Albacore" test results all slopes are negative, but the magnitudes vary. Appearances are that scale effects nearly disappear at a Reynolds number of approximately 7.4×10^7, which, however, is equivalent to a 70-foot model being driven at a speed-length ratio of 0.8. Obviously, it is not practical to test 70-foot models.

Further research is needed in the area of scale effects on propulsion factors. So far all such research has been performed on ship

hull-forms of specific designs, in which cases fullness, aperture clearance, etc. have been predetermined arbitrarily because of the convenience in choosing the form tests. However, it is here contended that individual components contributing to scale effects must be studied. Theoretical analyses, such as that by Tsakonas, should be further developed and then verified experimentally. The calculations by Tsakonas show a constant slope in wake-fraction and thrust deduction with increasing Reynolds number, which is not to be expected from the single consideration that the negative slope of the friction lines is always decreasing. Hence, three dimensional boundary layer theory should be developed further and tests run on propelled bodies of revolution generated from known singularity distributions.

It is also advocated that scale effect on potential flow be investigated from the viewpoint that boundary layer scale effect automatically alters the potential flow field. Lastly, viscosity effects on dissipation of waves, hence wave wake, should be further investigated.

Without concentrated effort as outlined above, further geosim testing can only lead to more ambiguous and contradictory results.

TABLE I

Series 60, C_B = .60, LBP = 600 feet
U of M: Model No. 912, Propeller No. 1, λ = 42.857
DTMB: Model No. 4210, Propeller No. 3378, λ = 30.000

	0.6		0.7		0.8		0.9	
$V/\sqrt{L_{BP}}$	UM	TMB	UM	TMB	UM	TMB	UM	TMB
SHP	5500	5500	9000	9000	13200	13200	23200	23200
RPM	62	64	73	76	85	87	100	103
w	.28	.26	.26	.25	.25	.23	.25	.24
t	.18	.15	.19	.16	.19	.17	.19	.17
e_r	1.03	1.01	1.04	1.00	1.04	1.02	1.04	1.01
e_h	1.14	1.15	1.10	1.12	1.08	1.08	1.08	1.09
EHP/SHP	.80	.80	.77	.77	.77	.78	.74	.74

		UM	TMB
e_p	at J = .76	.64	.69

Note: The pitch of Propeller No. 1 was 6% higher than that of Propeller No. 3378.

TABLE II

Series 60, C_B = .75, LBP = 600 feet
U of M: Model No. 913, Propeller No. 2, λ = 42.857
DTMB: Model No. 4213, Propeller No. 3379, λ = 30.000

	0.5		0.6		0.7		0.8	
$V/\sqrt{L_{BP}}$	UM	TMB	UM	TMB	UM	TMB	UM	TMB
SHP	4300	4300	8100	7700	14500	14500	31700	31700
RPM	50	50	61	61	73	74	92	94
w	.35	.31	.35	.31	.37	.29	.35	.27
t	.20	.16	.20	.17	.22	.18	.22	.16
e_r	1.03	1.04	1.04	1.01	.96	1.01	1.01	1.01
e_h	1.23	1.22	1.23	1.20	1.24	1.19	1.20	1.25
EHP/SHP	.80	.81	.79	.80	.75	.77	.71	.71

	UM	TMB
e_p at J = .62	.63	.62

Note: The pitch of Propeller No. 2 was 2% higher than that of Propeller No. 3379.

TABLE III

Series 60, C_B = .80, LBP = 600 feet
U of M: Model No. 932, Propeller No. 4, λ = 42.857
DTMB: Model No. 4214-B4, Propeller No. 3377, λ = 30.000

	0.4		0.5		0.6		0.7	
$V/\sqrt{L_{BP}}$	UM	TMB	UM	TMB	UM	TMB	UM	TMB
SHP	2600	2500	4900	4900	9500	9400	20400	20200
RPM	40	42	49	52	62	65	79	83
w	.39	.36	.39	.35	.38	.35	.36	.31
t	.22	.17	.22	.19	.22	.20	.21	.19
e_r	1.01	1.00	1.01	1.01	.99	1.01	1.00	1.02
e_h	1.28	1.30	1.28	1.25	1.26	1.23	1.23	1.18
EHP/SHP	.82	.82	.80	.80	.78	.78	.73	.74

	UM	TMB
e_p at J = .58	.63	.62

Note: The pitch of Propeller No. 4 was 5% higher than that of Propeller No. 3377.

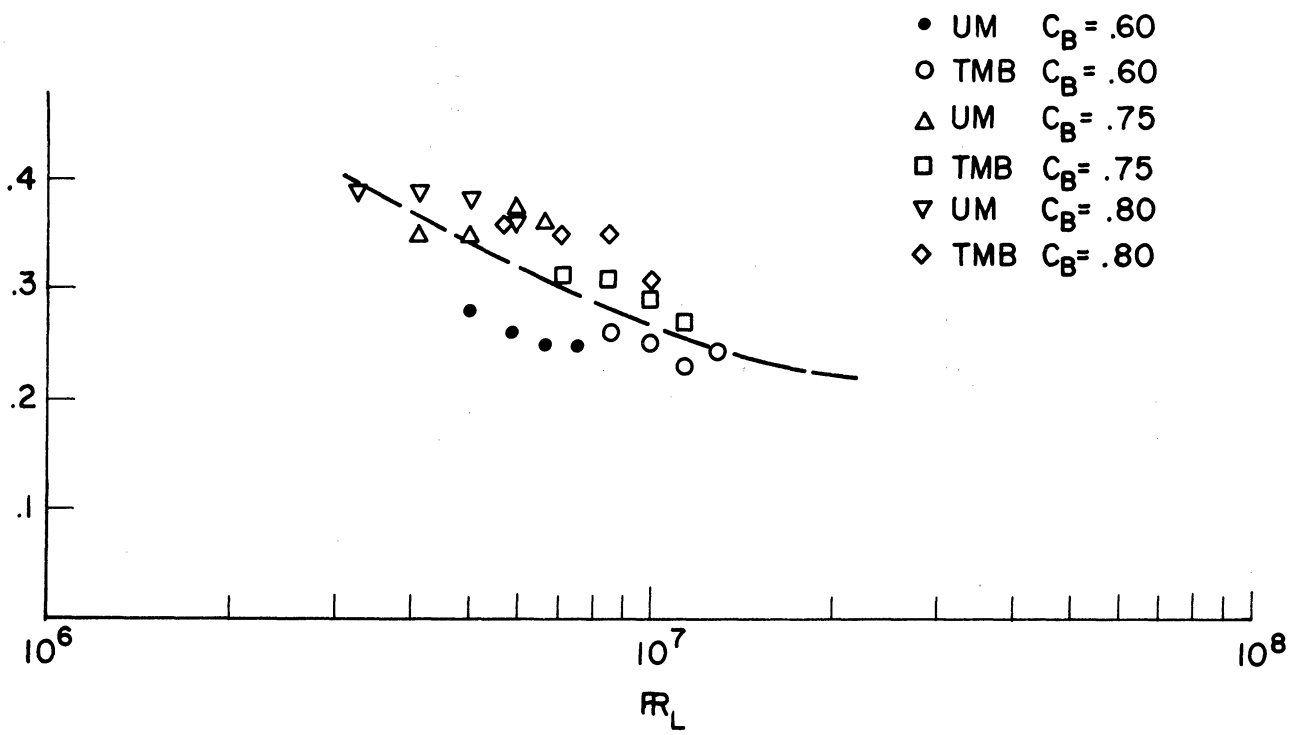

Figure 5. Mean wake fraction values of DTMB and U of M for three series 60 parents.

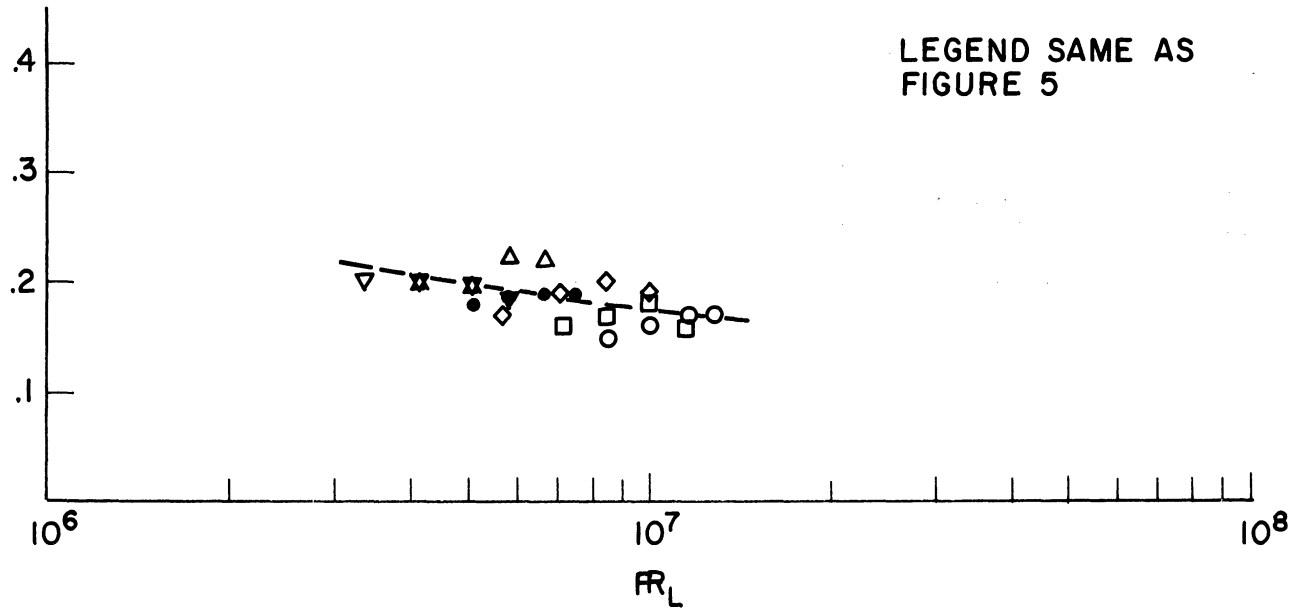

Figure 6. Thrust deduction values of DTMB and U of M for three series 60 parents.

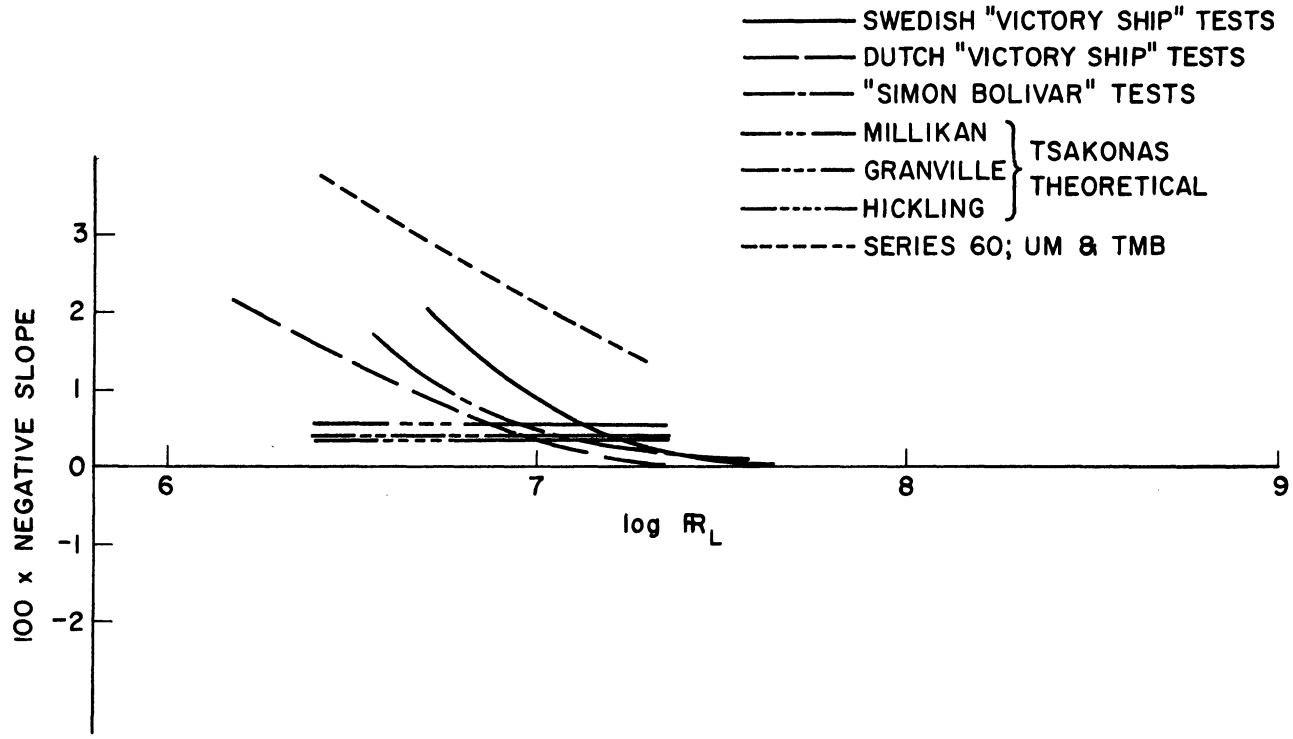

Figure 7. Mean wake fraction scale effect expressed as negative slope of lines plotted in previous figures.

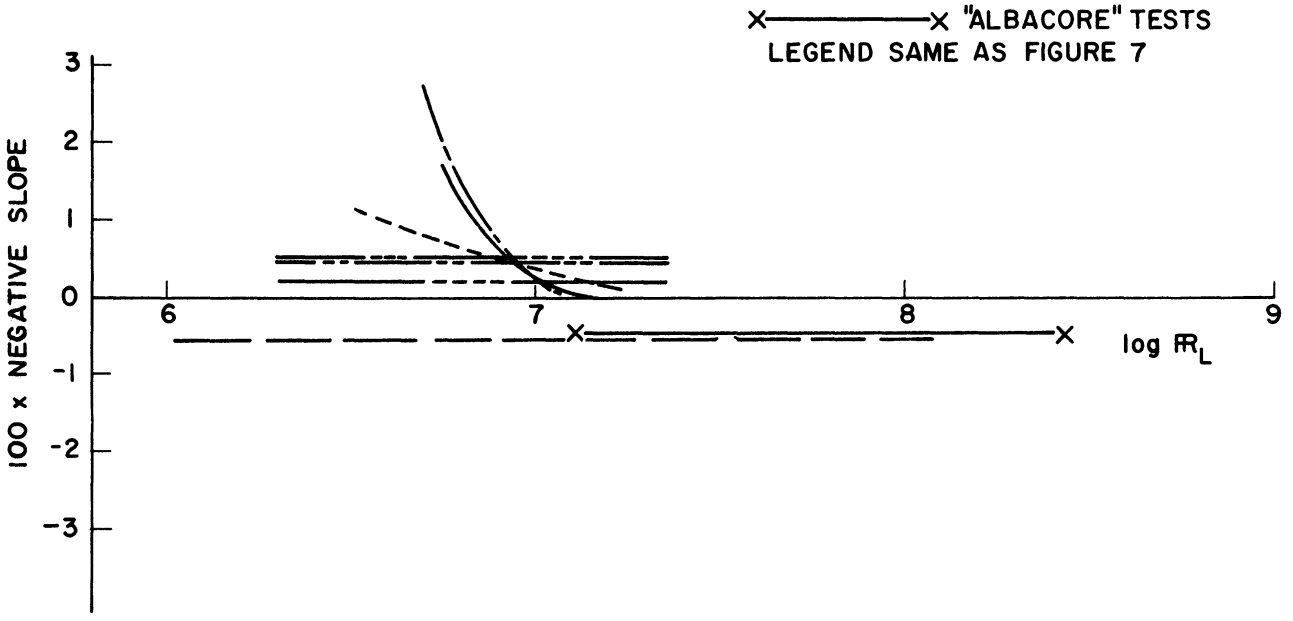

Figure 8. Thrust deduction scale effect expressed as negative slope of lines plotted in previous figures.

BIBLIOGRAPHY

1. Hill, J. G. "Scale Effect on Self Propulsion Factors." DTMB Report 731, Sept., 1950.

2. Tsakonas, S. and W. R. Jacobs. "Potential and Viscous Parts of the Thrust Deduction and Wake Fraction for an Ellipsoid of Revolution." Journal of Ship Research, Vol. 4, No. 2.

3. Tsakonas, S., W. Jacobs and J. Breslin. "Wake Fraction and Thrust Deduction Scale Effects." Davidson Laboratory Note No. 595, presented at Ninth International Towing Tank Conference.

4. Van Manen, J. D. and A. J. W. Lap. "Scale-Effect Experiments on Victory Ships and Models: Part II. - Analysis of Wake Measurements on a Model Family and the Model Family and the Model Boat 'D. C. Endert Jr.'." Transactions of R.I.N.A., Vol. 100, 1958.

5. Van Lammeren, W. P. A., J. D. Van Manen, and A. J. W. Lap. "Scale Effect Experiments on Victory Ships and Models: Part I. - Analysis of the Resistance and Thrust-Measurements on a Model Family and on the Model Boat 'D. C. Endert, Jr.'." Transactions of R.I.N.A., Vol. 97, 1955.

6. Hadler, J. "Propulsion Scale Effects." Proceedings of the Eighth International Towing Tank Conference, Madrid, Spain, September, 1957.

7. Edstrand, H. "Propulsion Scale Effects." Proceedings of the Eighth International Towing Tank Conference, Madrid, Spain, September, 1957.

8. Van Lammeren, W. P. A. "Propulsion Scale Effect." Transactions of the North-East-Coast Institution of Engineers and Shipbuilders, 1939-40.

9. Michelsen, F. C., R. B. Couch and H. C. Kim. "Resistance and Propulsion Tests on Two Series 60 Models." University of Michigan ORA Report No. 03509-1-F, April, 1961.

10. Michelsen, F. C., R. B. Couch and H. C. Kim. "Resistance on Two Models - (1) Series 60, C_B = .80, (2) High Speed Cargo Ship PD108-55-0." University of Michigan ORA Report 04652-1-F.